

OPTIMAL LOW THRESHOLD TRAJECTORIES
USING DIFFERENTIAL INCLUSION CONCEPTS

by

VICTORIA COVERSTONE-CARROLL*

and

STEVEN N. WILLIAMS**

submitted to the

AIAA/AAS SPACE FLIGHT MECHANICS MEETING
COCA BEACH, FLORIDA

*Assistant Professor, Department of Aeronautical and Astronautical
Engineering, University of Illinois at Urbana-Champaign, Member AIAA, Member AAS

**Member of the Technical Staff, Mission Design Section, Jet Propulsion Laboratory,
California Institute of Technology, Pasadena, CA, Member AIAA.

OPTIMAL LOW THRUST TRAJECTORIES USING DIFFERENTIAL INCLUSION CONCEPTS

Victoria Coverstone-Carroll
Steven N. Williams

A direct optimization method based on differential inclusion concepts has been developed and used to compute low thrust trajectories. This new formulation removes explicit control dependence from the problem statement thereby reducing the dimension of the parameter space of the resulting nonlinear programming problem. A simple example of a two-dimensional gravity-free trajectory involving a maximum velocity transfer to a rectilinear path is discussed. Three interplanetary trajectory examples, an Earth-Mars constant specific impulse transfer, an Earth-Jupiter constant specific impulse transfer, and an Earth-Venus-Mars variable specific impulse gravity assist, are also included. An evaluation of the technique's performance is provided.

Introduction

Low thrust electric propulsion systems typically have their greatest benefit for high energy planetary missions. Missions that have been examined include main belt asteroid rendezvous, comet rendezvous, outer planet and Mercury orbiters, Pluto flyby and solar probe missions. Most low thrust mission design software use calculus-based algorithms that can be subdivided into two main classes: indirect and direct. The indirect approach uses the calculus of variations to obtain a set of necessary conditions whose solution ensures a local extremum of the objective function. In contrast, direct methods use gradients of the objective function to search the parameter space and locate a local extremum. Direct methods often transform optimal control problems into nonlinear programming problems (NLP). With these methods, finite approximations to the state differential equations are exploited. The objective function is then directly minimized by varying discrete values for the states and controls.

A direct method based on differential inclusion concepts has been developed and used to compute low thrust trajectories. This new formulation removes explicit control dependence from the problem statement thereby reducing the dimension of the parameter space for the NLP. As a consequence of eliminating the control parameters, fewer nonlinear constraints are required to represent the dynamics of the problem.

Problem Statement

The equation of motion for a spacecraft subject to a single gravitational source is given through the rocket equation?

$$\ddot{\mathbf{r}} = \mathbf{g}(\mathbf{r}) + \frac{T}{m} \hat{\mathbf{u}} = \mathbf{g}(\mathbf{r}) + \mathbf{1}'' \quad (1)$$

where \mathbf{r} is the position vector, $\mathbf{g}(\mathbf{r})$ the gravitational force per unit mass vector, T the engine thrust, $\hat{\mathbf{u}}$ a unit vector in the thrust direction, $\mathbf{1}''$ the thrust per unit mass vector and m the vehicle mass. The model used for the spacecraft's propulsion system, whether constant specific impulse (csi) or variable specific impulse (vsi), directly affects the relationship between control effort and propellant consumption. The equations that govern the change in mass for both csi and vsi systems are given below. The variable c is the propellant's exhaust velocity.

$$\text{csi case:} \quad \frac{dm}{dt} = -\frac{T}{c} \quad (2)$$

$$\text{vsi case:} \quad \frac{d}{dt}\left(\frac{1}{m}\right) = \frac{I^2}{2P} \quad (3)$$

The mass-control relationships described above may be written in a variety of equivalent ways. The expressions shown in equations (2) and (3) are chosen to simplify the following derivation. Define a state vector \mathbf{x} that for the csi case is $\mathbf{x}^T = [\mathbf{r}^T \ \mathbf{v}^T \ \gamma]$ where \mathbf{v} is the velocity vector and $\gamma = \ln(m)$ and for the vsi case is $\mathbf{x}^T = [\mathbf{r}^T \ \mathbf{v}^T \ \alpha]$ where $\alpha = \frac{P}{m}$. The state rates for the two systems are then obtained through equations (1)-(3),

$$\dot{\mathbf{r}} = \mathbf{v} \quad (4)$$

$$\text{csi case:} \quad \dot{\mathbf{v}} = \mathbf{g}(\mathbf{r}) - I' \exp(-\gamma) \hat{\mathbf{u}} \quad (5)$$

$$\frac{d\gamma}{dt} = -\frac{I' \exp(-\gamma)}{c} \quad (6)$$

$$\dot{\mathbf{r}} = \mathbf{v} \quad (7)$$

$$\text{vsi case:} \quad \dot{\mathbf{v}} = \mathbf{g}(\mathbf{r}) + \mathbf{1}'' \quad (8)$$

$$\frac{d\alpha}{dt} = \frac{I'^2 I'}{2} \quad (9)$$

To determine an optimal trajectory, controls ($\Gamma\hat{u}$ or l) must be chosen to satisfy any boundary conditions on the states while minimizing an objective function.

Recently, it has been shown that many **optimal** control problems can be described by functional differential inclusions.³⁻⁶ Differential inclusions represent the dynamics of a problem in terms of attainable sets rather than differential equations. Seywald⁶ demonstrated how differential inclusions could be used to solve one-dimensional trajectory optimization problems. Examination of equations (4)-(6) and (7)-(9) show that $\frac{dy}{dt}$ and $\frac{d\alpha}{dt}$ contain information about the control magnitude but not the control direction, so for three-dimensional trajectories where a control direction is needed, representing the problem with differential inclusions is not straight-forward, however, if the \dot{v} equations are manipulated to produce a scalar equation of the form given in equations (10)-(11), explicit appearance of the control is removed from the differential equations.

$$\text{csi case:} \quad (\dot{v} - g(r))^T (\dot{v} - g(r)) = \left(\frac{dy}{dt}\right)^2 c^2 \quad (10)$$

$$\text{vsi case:} \quad (\dot{v} - g(r))^T (\dot{v} - g(r)) = 2\delta \quad (11)$$

This simple manipulation has eliminated the control variables from the problem statement and replaced them with a nonlinear scalar constraint on the states and state rates. The reduced-order problem consisting of equations (4), (6) and (10) for csi and (7), (9) and (11) for vsi can be formulated as a nonlinear programming problem (NLP). To convert to the NLP form, the total maneuver time is divided into N segments. The end points of each segment are defined as the left and right nodes and denoted by subscripts l and r. Equal segment lengths t_s are assumed and first-order approximations are used for the derivatives across each segment. State rates are represented as:

$$\dot{r} \cong \frac{r_r - r_l}{t_s} \quad \dot{v} \cong \frac{v_r - v_l}{t_s} \quad \frac{dy}{dt} \cong \frac{y_r - y_l}{t_s} \quad \text{and} \quad \frac{d\alpha}{dt} \cong \frac{\alpha_r - \alpha_l}{t_s} \quad (12)$$

The position derivative approximation given above is substituted into equations (4) and (7) and the equation is evaluated at the segment center yielding 3 linear equality constraints for each segment. A total of 3N linear equality constraints are needed for the total trajectory. Fixed time t_f maneuvers are assumed, therefore $t_s = t_f/N$.

$$\mathbf{r}_r - \mathbf{r}_1 - \frac{(\mathbf{v}_r + \mathbf{v}_1)t_s}{2} = \mathbf{0} \quad (13)$$

The nonlinear scalar constraint given in equations (10) and (11) is evaluated at the segment center and becomes the nonlinear equality constraint below. A total of N nonlinear constraints are required for the entire maneuver.

$$\text{csi case:} \quad (\mathbf{v}_r - \mathbf{v}_1 - \mathbf{t}_s \mathbf{g}(\mathbf{r}_c))^T (\mathbf{v}_r - \mathbf{v}_1 - \mathbf{t}_s \mathbf{g}(\mathbf{r}_c)) - 2c^2(\gamma_r - \gamma_1)^2 = 0 \quad (14)$$

$$\text{vsi case:} \quad (\mathbf{v}_r - \mathbf{v}_1 - \mathbf{t}_s \mathbf{g}(\mathbf{r}_c))^T (\mathbf{v}_r - \mathbf{v}_1 - \mathbf{t}_s \mathbf{g}(\mathbf{r}_c)) - 2t_s(\alpha_r - \alpha_1) = 0 \quad (15)$$

$$\text{where } \mathbf{r}_c = \frac{\mathbf{r}_1 + \mathbf{r}_r}{2}$$

The mass-related variables (γ, α) evolve subject to the following nonlinear and linear inequality constraints. The inequality constraints demonstrate the differential inclusion concept of a state rate being contained in a set rather than being dictated by a differential equality constraint. Note that this formulation does not assume a control structure for the csi case. The control structure for the trajectory is contained in their values.

$$\text{csi case:} \quad 0 \leq -(\gamma_r - \gamma_1) \exp\left(\frac{\gamma_r + \gamma_1}{2}\right) c \leq T t_s \quad (16)$$

$$\text{csi case:} \quad \gamma_r - \gamma_1 \leq 0 \quad (17)$$

$$\text{vsi case:} \quad 0 \leq \alpha_r - \alpha_1 < \infty \quad (18)$$

A Simple Example

For illustrative purposes, a simple two-dimensional gravity-free csi example that involves a maximum velocity transfer to a rectilinear path is discussed. This problem was selected because the solution can be obtained analytically through the indirect approach outlined in Bryson and Ho [7]. Bryson and Ho formulate the problem in terms of thrust acceleration where in this formulation the thrust magnitude divided by the current mass is used. The optimal solution consists of a constant thrust magnitude T and a time-varying control angle $\beta(t)$ described by the well-known bilinear tangent steering law. The problem statement is to transfer a particle from rest at the origin to a path parallel to the x-axis a distance h away in a given time t_f arriving with zero velocity in the y direction and

maximum velocity in the x direction. The following conditions were placed on the transfer. The initial mass of the vehicle $m(t_0)$, assumed to consist of only propellant, was set to unity. The thrust magnitude and the total maneuver time t_f were also set to unity. The vertical distance h was chosen to be 0.1 and the total number of segments N used to discretize the trajectory was selected as 10.

Figures 1-4 display some characteristics of the optimal trajectory. Figure 1 shows the trajectory, Figure 2 the velocity profile, and Figure 3 the propellant mass history. Cases were also run with a limit on the propellant mass and the optimal solution used all available propellant to maximize its final velocity. Figure 4 contains two curves for the control angle β . As described in [7], indirect methods show that the optimal control angle is given by the bilinear tangent steering law given by equation (19). The values of the constants for this problem are $c_1 = -3.38 \times 10^{-5}$, $c_2 = -3.68 \times 10^{-2}$, $c_3 = -1.00 \times 10^{-1}$, and $c_4 = -2.87 \times 10^{-2}$. Using these numbers, equation (19) was used to calculate the control angle at the segment endpoints.

$$\tan(\beta) = \frac{-c_2 t + c_4}{-c_1 t + c_3} \quad (19)$$

The second curve comes from post-processing the output from the differential inclusion NIP and is plotted at the segment centers. If the approximations for the velocity rate of change shown in equation (12) are used, the control angle from the differential inclusion approach is calculated through the equation $\beta = \tan^{-1}(v_y/v_x)$. The two curves, one supplied through an indirect method and the other through a direct method, verify that the two solutions are nearly identical,

Interplanetary Trajectories

Motivation

The ultimate goal of this research is to develop a technique which can be used to identify potential trajectories for low thrust missions. When planning conventional interplanetary missions (using chemical propulsion), there is a wide array of tools and techniques available to design trajectories. Typically, trajectories are developed through a series of steps beginning with simple conic approximations treating planets as point masses and eventually including an optimization of deep space maneuver times and planetary flybys. There may or may not be intermediate steps using multi-conics, but the process

typically concludes with a numerical integration which incorporates a force model that may include multi-body gravitational effects, spherical harmonics, drag, solar pressure, and even relativistic effects. Generally, each step of the process is accomplished with a different piece of software.

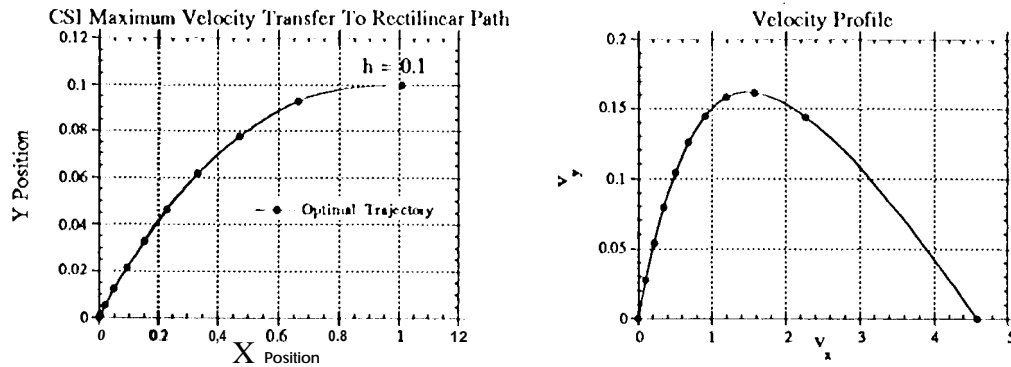


Figure 1-2: Position and Velocity Profiles

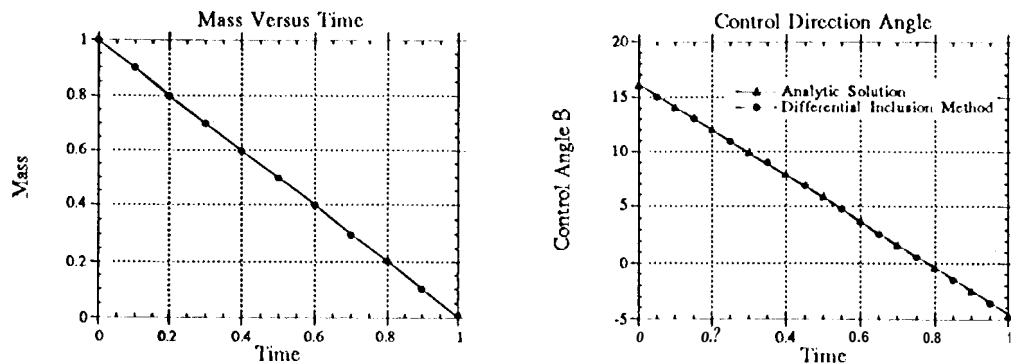


Figure 3-4: Mass and Control Angle Versus Maneuver Time

Unfortunately, a similar array of software tools for designing low thrust missions does not yet exist. One reason is that low-thrust trajectories are inherently more difficult to model. Instead of a discrete set of maneuvers and planetary encounters, a thrust direction and magnitude must be optimized at each instant to minimize the objective function (or maximize final mass). Low thrust trajectories at JPL are computed with the VARIABLE thrust Trajectory Optimization Program (VARITOP). This program is a general purpose two-body, sun-centered, low-thrust trajectory optimization and analysis program intended for preliminary mission feasibility studies. It optimizes the trajectory by solving a two-point boundary value problem (TPBVP) that involves numerical integration of the state and costate equations. VARITOP is a well established program which has been used since the

early 1960s. It is used in this paper as a standard with which to compare the results obtained with the differential inclusion approach. VARITOP contains several propulsion models, but the primary concern here is with the variable specific impulse (vsi) and constant specific impulse (csi) models. For the csi cases it is also important to distinguish between a constant power source (such as nuclear) and a variable source (such as solar electric). Only the constant power option is addressed in this paper.

Examples of both vsi and csi trajectories, comparing results between the differential inclusion (DI) technique and VARITOP follow. It is hoped that the role that DI will play in the future is as a preliminary design tool - not unlike the way conics are used for impulsive trajectories. One of the undesirable characteristics of using an indirect approach (VARITOP), is that a "starting guess" for the Lagrange multipliers that correspond to the initial state must be determined. It is sometimes useful to associate a region of convergence with the initial multiplier estimates. If the initial estimates are outside this region, it may be very difficult to achieve a converged solution with VARITOP. The DI technique does not require an estimate of Lagrange multipliers, but may be used to generate these multipliers, thereby providing very good initial starting conditions for VARITOP.

Initial Lagrange Multiplier Generation

The nonlinear programming problem (NLP) software NPSOL, Version 4.0⁸ was used to obtain the differential inclusion mission scenarios described in the next section. Upon converging to a finite-dimensional approximation of the optimal solution, NPSOL provides estimates on how constraining variables affect the optimal objective function. In the following mission scenarios, the initial position and velocity have been specified. Hamilton-Jacobi theory states that on the optimal trajectory, the costate (Lagrange multipliers) is the sensitivity of the objective function with respect to the states,⁷ and therefore initial costates are available from NPSOL. If any initial condition is not specified but allowed to be optimized, the initial value of the corresponding costate is zero.

Trajectory Examples

Three examples are shown that exercise various aspects of the differential inclusion (DI) approach. The first is an Earth-Mars csi trajectory. It is a fairly straightforward case, but includes a large coast arc. It is significant that the DI approach accurately models this coast arc. The second example shown is a csi Earth-Jupiter trajectory which demonstrates that this approach may be used for outer solar system trajectories with their longer flight

times. The final case is a vsi Earth-Venus-Mars trajectory and demonstrates the ability to model planetary gravity assists.

Figure 5 shows the trajectories for the csi Earth-Mars rendezvous computed by the DI and VA RITOP software. The spacecraft departs Earth on November 19, 1994 with Earth's orbital velocity. A rendezvous with Mars occurs 184 days later on May 22, 1995. A constant power source of 450 kW and a specific impulse of 4860 seconds is used, For the DI approach, the total transfer time was divided into 20 segments. The finite approximation of the DI approach computes a coasting interval (denoted by dots) between January 12 through March 2.8. The VARITOP solution includes a coast arc that begins on January 10, 1995 and terminates on March 27, 1995. The two coasting periods differ by only a few days. In each case, the spacecraft began the transfer with an initial mass of 10,000 kg. VARITOP computes a final mass of 7185 kg where DI finishes with 7149 kg. The DI approach gives an excellent first-order approximation to the continuous optimal solution.

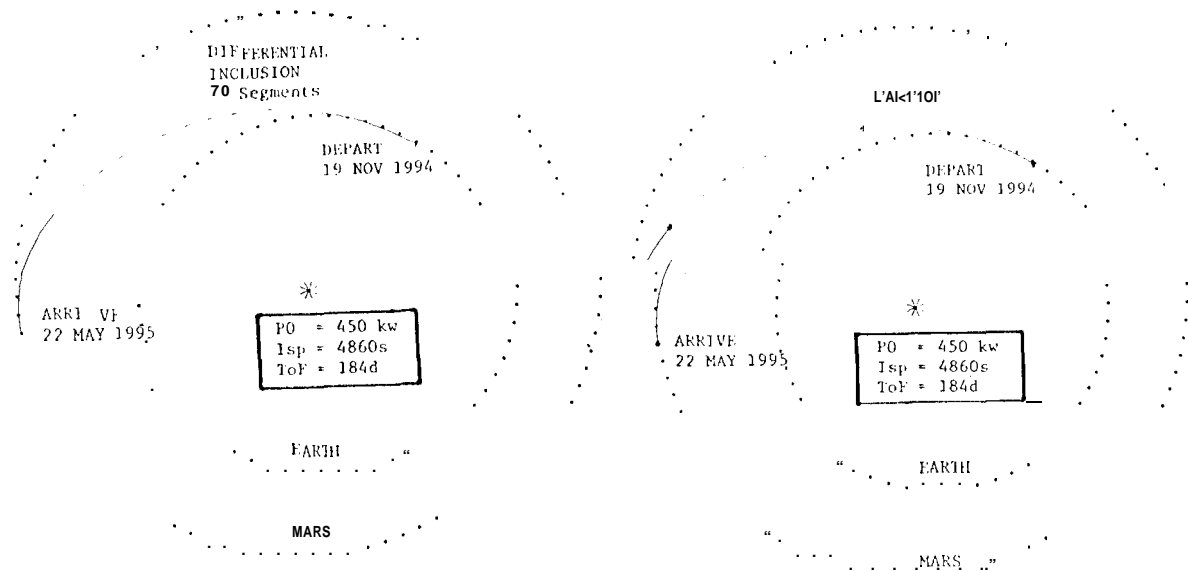


Figure 5: Earth-Mars CSI Trajectories From DI (left) and VARITOP (right)

The next example shown in Figure 6 is an Earth-Jupiter csi 680 day transfer. Due to the larger transfer time, 30 segments were used for the DI formulation. The spacecraft departs Earth on May 25, 2001, burns continuously until July 5, 2002, has a brief coast period until August 8, 2002, and then burns until the rendezvous with Jupiter on April 5,

2003. The power source supplies 115 kW and the propulsion system has a specific impulse of 4000 seconds. The DI software computed a coasting period of only 2 days beginning on July 28, 2002. This coasting arc is too small to be detected on the plot. Both trajectories began with an initial mass of 10,000 kg. VARITOP obtained a final mass of 3798 kg and DI 3526 kg. The flight time for this trajectory is more than 3.5 times as long as the previous Mars trajectory. One might expect that as flight times get longer, the DI formulation will experience problems because the larger segments give a less accurate representation of the trajectory. This was not a problem in this case. Figure 6 shows quite good agreement between the two different approaches. Some experimentation was done with Pluto trajectories and these seemed to be more sensitive to this effect,

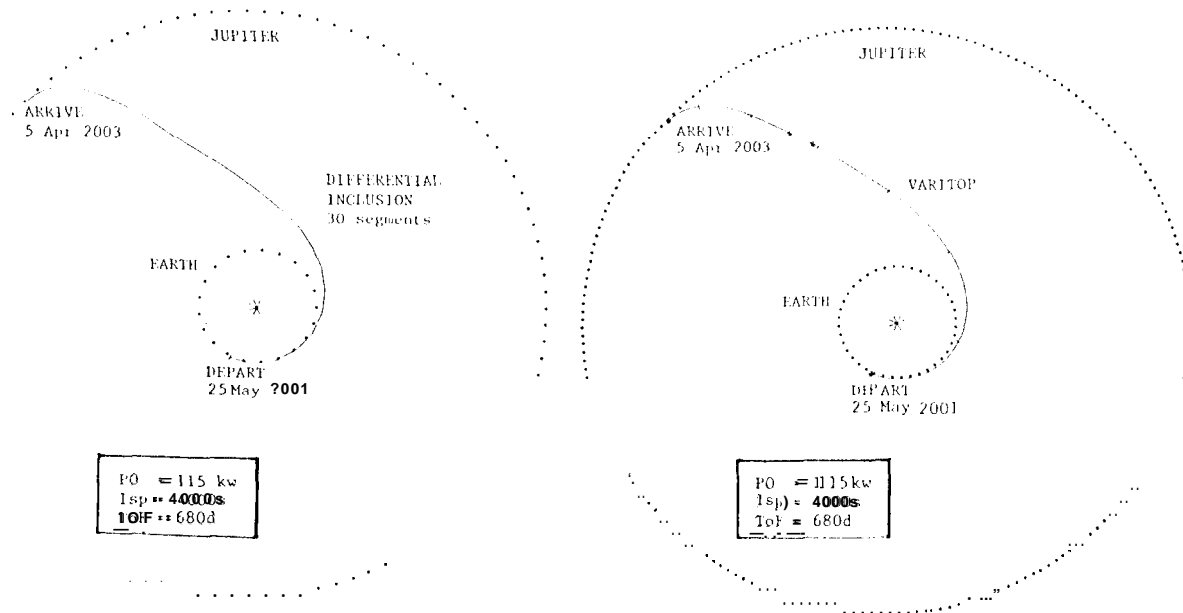


Figure 6: Earth-Jupiter CSI Trajectories from DI (left) and VARITOP (right)

The final trajectory shown in Figure 7 is a Venus-Mars trajectory with an unpowered gravity assist at Venus. The spacecraft departs on January 1, 2001, flies by Venus on May 10 and rendezvous with Mars on March 21, 2003. In each case, the initial mass is 5,000 kg and the power source provides 33.9 kW. For the DI approach, each leg of the transfer was divided into 40 segments. Note that in Figure 7 the discrete nature of the DI approach is apparent after the flyby of Venus when the spacecraft is traveling at a higher speed. The final mass predicted by DI was 3532 kg while VARITOP predicted 3577 kg.

The modeling of a planetary flyby requires the addition of two nonlinear equality constraints for each flyby. Since only unpowered flybys are considered, the first constraint states that the magnitude of the spacecraft velocity with respect to the flyby body v_∞ is constant. In equation (20), \mathbf{v}^{In} and \mathbf{v}^{Out} are the heliocentric velocities before and after the flyby. The planet's heliocentric velocity is denoted by \mathbf{v}_p .

$$v_\infty^{\text{In}} = v_\infty^{\text{Out}} \Rightarrow (\mathbf{v}^{\text{In}} - \mathbf{v}_p)^T (\mathbf{v}^{\text{In}} - \mathbf{v}_p) - (\mathbf{v}^{\text{Out}} - \mathbf{v}_p)^T (\mathbf{v}^{\text{Out}} - \mathbf{v}_p) = 0 \quad (2.0)$$

The second constraint relates the flyby radius R of the spacecraft from the body to the turning angle δ . The flyby body's gravitational constant is denoted by μ .

$$\delta = 2 \sin^{-1} \left(\frac{1}{1 + \frac{R v_\infty^2}{\mu}} \right) = \cos^{-1} \left(\frac{\mathbf{v}^{\text{In}} \cdot \mathbf{v}_p}{v_\infty^2} \frac{(\mathbf{v}^{\text{Out}} \cdot \mathbf{v}_p)}{v_\infty^2} \right) \quad (21)$$

Using trigonometric identities on equation (21), the following constraint results.

$$\mu \left[\frac{2 v_\infty^2}{v_\infty^2 - (\mathbf{v}^{\text{In}} \cdot \mathbf{v}_p)^T (\mathbf{v}^{\text{Out}} \cdot \mathbf{v}_p)} \right] - \mu - v_\infty^2 R = 0 \quad (22)$$

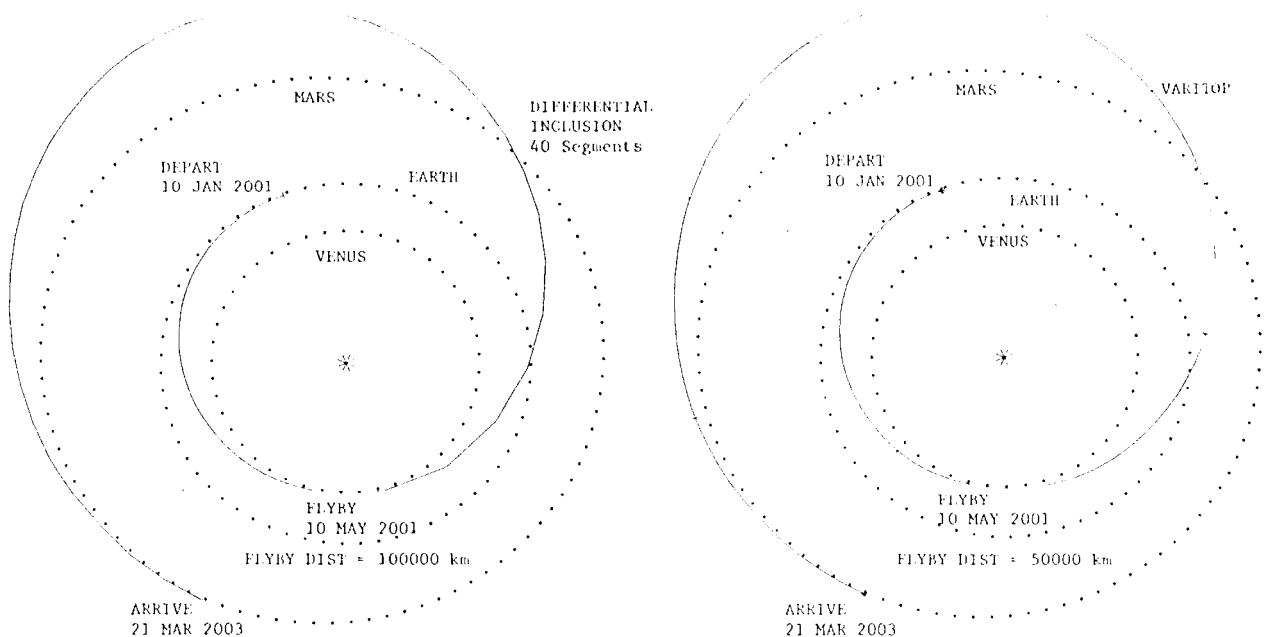


Figure 7: Earth-Venus-Mars VSI Trajectories From DI (left) and VARITOP (right)

To use VARITOP to compute flyby trajectories, create values are required after each gravity assist. Since the position of the intermediate body is specified, the value of the costate conjugate to the position is supplied by the NLP solver. However, the costate to the velocity is not available since the incoming and outgoing velocity is to be optimized subject to the two constraints given in equation (20) and (22). Therefore, optimal control theory is used to calculate an estimate for the velocity costate λ_v . Costate estimates from the converged differential inclusion code were used to initiate VARITOP for the Earth-Venus-Mars trajectory.

$$\lambda_v = g(r) - \frac{v_r - v_l}{t_s} \quad (23)$$

Conclusions & Recommendations for Future Work

This paper discusses a technique for calculating optimal low-thrust trajectories using a finite dimensional approximation to the continuous time problem. The differential inclusion technique formulates a nonlinear programming problem (NLP) where the control parameters are eliminated resulting in a scalar constraint on the states and state rates. The parameter space of the resulting NLP is thereby reduced over other direct methods.

The VARITOP trajectories shown in this paper were obtained using the initial Lagrange multiplier estimates from the differential inclusion (DI) solution. A significant advantage of using the DI software to obtain initial Lagrange multipliers for VARITOP is that the user can walk away from the computer and work on something else while the DI code runs. Using VARITOP alone with only the user's best guess for the initial multipliers may take as long if not longer to obtain the same results as the DI/VARITOP combination, however, the user's entire attention must be given to VARITOP due to its interactive nature. The drawback to using DI alone is its finite approximation to the continuous problem. To increase the accuracy of the differential inclusion solution, the number of segments can be increased but this will be at the expense of computation time required to obtain a solution.

We believe that the DI approach offers a powerful new technique for computing low thrust trajectories. Results demonstrate good agreement with established methods for a variety of missions. In the future, the technique will be expanded to include a variable power source so that missions such as solar electric maybe examined. Also, strategies for reducing the computation time will be explored.

Acknowledgments

The research described in this paper was carried out by the Jet Propulsion Laboratory, California Institute of Technology, under a contract with the National Aeronautics and Space Administration.

References

1. Sauer, C. G. Jr., "Planetary Mission Performance for Small Solar Electric Propulsion Spacecraft", AAS Paper 93-561, AAS/AIAA Astrodynamics Specialist Conference, August 16-19, 1993, Victoria, B.C, Canada.
2. Prussing, J. II. and B.A. Conway, Orbital Mechanics, Oxford University Press, New York, 1993.
3. Kisielewicz, M., Differential inclusions and Optimal Control, Kluwer Academic Publishers, Boston, 1991.
4. Aubin, J.-P., Viability Theory, Krihauser, Boston, 1991.
5. Deimling, K., Multivalued Differential Equations, Walter de Gruyter, Berlin, 1992.
6. Seywald, H., "Trajectory Optimization Based on Differential Inclusion", AAS Paper 93-148, AAS/AIAA Spaceflight Mechanics Meeting, February 22-24, 1993, Pasadena, California.
7. Bryson, A. and Ho, Y.-C., Applied Optimal Control, Hemisphere Publishing Corporation, New York, 1975.
8. Gill, P.E., Murray, W., Saunders, M.A. and M.H. Wright, "User's Guide for NPSOL (Version 4.0): A Fortran Package for Nonlinear Programming"; Technical Report S01. 86-2, January 1986.